

# Final stage of merging binaries of supermassive black holes: observational signatures

Jian-Min Wang<sup>1,2,3\*</sup>, Yu-Yang Songsheng<sup>1,2</sup>, Yan-Rong Li<sup>1</sup> and Pu Du<sup>1</sup>

<sup>1</sup>Key Laboratory for Particle Astrophysics, Institute of High Energy Physics, Chinese Academy of Sciences, 19B Yuquan Road, Beijing 100049, China

<sup>2</sup>School of Astronomy and Space Science, University of Chinese Academy of Sciences, 19A Yuquan Road, Beijing 100049, China

<sup>3</sup>National Astronomical Observatories of China, The Chinese Academy of Sciences, 20A Datun Road, Beijing 100020, China

## ABSTRACT

There are increasing interests in binary supermassive black holes (SMBHs), but merging binaries with separations smaller than  $\sim 1$  light days ( $\sim 10^2$  gravitational radii for  $10^8 M_\odot$ ), which are rapidly evolving under control of gravitational waves, are elusive in observations. In this paper, we discuss fates of mini-disks around component SMBHs for three regimes: 1) low rates (advection-dominated accretion flows: ADAFs); 2) intermediate rates; 3) super-Eddington accretion rates. Mini-disks with intermediate rates are undergoing evaporation through thermal conduction of hot corona forming a hybrid radial structure. When the binary orbital periods are shorter than sound propagation timescales of the evaporated mini-disks, a new instability, denoted as sound instability, arises because the disks will be highly twisted so that they are destroyed. We demonstrate a critical separation of  $A_{\text{crit}} (\sim 10^2 R_g)$  from the sound instability of the mini-disks and the cavity is full of hot gas. For those binaries, component SMBHs are accreting with Bondi mode in the ADAF regime, showing periodic variations resulting from Doppler boosting effects in radio from the ADAFs due to orbital motion. In the mean while, the circumbinary disks (CBDs) are still not hot enough (ultraviolet deficit) to generate photons to ionize gas for broad emission lines. For slightly super-Eddington accretion of the CBDs, Mg II line appears with decreases of UV deficit, and for intermediate super-Eddington Balmer lines appear, but C IV line never unless CBD accretion rates are extremely high. Moreover, if the CBDs are misaligned with the binary plane, it is then expected to have optical periodical variations with about ten times radio periods.

**Key words:** galaxies: active – quasars: general – quasars: supermassive black holes

## 1 INTRODUCTION

Searching for binaries of supermassive black holes (SMBHs) in galactic centers draw much attention not only for galaxy formation and evolution but also for detection of low-frequency gravitational waves through Pulsar Timing Array (PTA). As natural consequence of galaxy mergers, binary SMBHs evolve through different phases (e.g., Begelman et al. 1980; Milosavljević & Merritt 2001; Volonteri et al. 2009), however, those close binaries of SMBHs (CB-SMBHs: separations less than 0.1 pc) are still elusive in observations (Wang & Li 2020; Bogdanović et al. 2021). There are many characteristics of CB-SMBHs from broad emission lines (Popović 2012; De Rosa et al. 2019; Bogdanović et al. 2021; Charisi et al. 2022) even more clues from observational evidence from shifting broad emission line, mass deficits in density profile of galactic nuclei, UV continuum deficit, reverberation mapping signals to interferometric signals of GRAVITY/VLTI, gas dynamics of circumbinary disks, to polarized spectra (Wang & Li 2020), but it is hard to draw conclusive remarks on individual candidates (Wang & Li 2020). Difficulties of identifying CB-SMBHs rest on lack of conclusive criterions. What are the key features of binary SMBHs at different stages in light of separations?

When the binary spirals in a stage with separations of  $\sim 10^4 R_g$  (where  $R_g = 1.5 \times 10^{13} M_8$  cm is gravitational radius,  $M_8$  is SMBH

mass in units of  $10^8 M_\odot$ ), the configurations of the binary SMBHs with accretion disks and broad-line regions (BLRs) are still independent of each other according to the  $R - L$  relation (Kaspi et al. 2000; Bentz et al. 2013; Du & Wang 2019). In this scale of separations, two SMBHs have their own BLRs and mini-disks (Shen & Loeb 2010). Identifying these binary SMBHs can be done by examining 2D transfer functions from reverberation mapping campaigns (Wang et al. 2018; Songsheng et al. 2020; Kovacévić et al. 2020a; Ji et al. 2021). The 2D transfer functions of binary BLRs rotating around each other will deliver binary information of the orbital motion (Wang et al. 2018), which are obviously different from a single BLR (e.g., Welsh & Horne 1991). A dedicated RM campaign of Monitoring AGNs with H $\beta$  Asymmetry (MAHA) for this goal has been undergoing through Wyoming Infrared Observatory (WIRO) 2.3m telescope (Du et al. 2018; Brotherton et al. 2020). Being different from this approach, long term campaigns of monitoring variations of profiles proceeds smoothly to test periodical shifts of red and blue peaks (Montuori et al. 2012; Decarli et al. 2013; Runnoe et al. 2017; Doan et al. 2020; Guo et al. 2019; Popović, et al. 2021). Moreover, GRAVITY/VLTI (Very Large Telescope Interferometer) with unprecedentedly high spatial resolution ( $\sim 10 \mu\text{as}$ ) has been applied to measure kinematics and spatial distributions of ionized gas of AGNs (GC 2017, 2018, 2020, 2021). This powerful tool has been first suggested by Songsheng et al. (2019) and Kovacévić et al. (2020b) to apply to close binaries of SMBHs. Combining

\* E-mail: wangjm@ihep.ac.cn

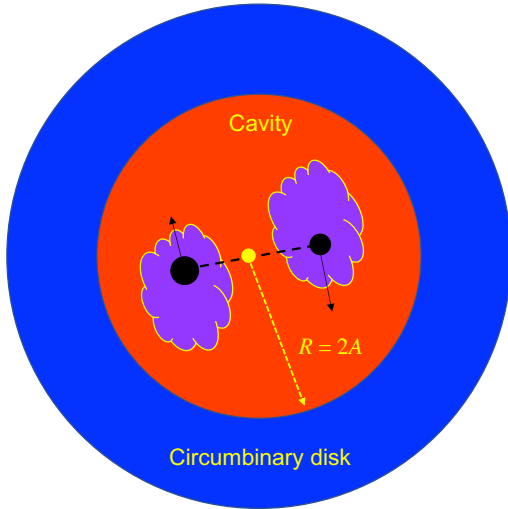


**Figure 1.** Carton of a merging binary of SMBHs with a circle orbit (separation is about  $10^2$  gravitational radius). Mini-disks around SMBHs are not able to survive so that a cavity is full of hot gas due to interaction with the binary. A circumbinary disk is then formed with a radius  $R \approx 2A$ . Each SMBH is accreting through Bondi mode from the cavity. Since SMBH Bondi accretion has low accretion rates, periodical variabilities in radio are expected due to orbital motion of the binary. See details in main text.

SpectroAstrometry (SA) and RM (hereafter SARM) offers an opportunity to identify them and measure orbital parameters of the binaries for testing nano-Hz gravitational waves, which is similar to that for cosmic distances (Wang et al. 2020).

Periodicity of AGNs receives much attention for candidates of CB-SMBHs in recent years. If the periodicity is caused by the binary SMBHs, separations of binaries with periods of a few years are about  $\sim 10^3 R_g$ . There are several long term campaigns of photometric surveys in time domain such as the Catalina Real-time Transient Survey (CRTS), Palomar/Zwicky Transient Factory (P/ZTF), Panoramic Survey Telescope and Rapid Response System (Pan-STARRS) and Dark Energy Survey (DES) for specific types of astronomical transients. There is growing evidence for periodical variations of optical light curves of AGNs from  $\sim 10$  year photometric campaigns for CB-SMBHs from CRTS (Graham et al. 2015b), from PFT (Charisi et al. 2016), from PanSTARRS (Liu et al. 2019), from DES Chen et al. (2020). Some of these periodic AGNs are likely not binary SMBHs since red-noise variabilities can generate periodic-like variations (e.g., Vaughan et al. 2016). There are also a few individual periodic AGNs, such as OJ 287 (Valtonen et al. 2008), PG 1302-102 (Graham et al. 2015a), NGC 5548 (Li et al. 2016) and Akn 120 (Li et al. 2019). Extremely eccentric CB-SMBHs with  $10^3 R_g$  separations merging fast may lead to changing-look events of AGNs (Wang & Bon 2020), however, such separations are still too large for GW to test gravitational waves in the chirping phase.

In this paper, we investigate the final stage of close binaries of SMBHs whose orbits are completely controlled by gravitational waves ( $\sim 10^2 R_g$ ). We show major physics of accretion onto such a close binary of SMBHs, and the peculiar spectral energy distributions of continuum. Moreover, the Doppler boosting effects due to fast orbital motion can be observed, and polarization observations are more useful (Dotti et al. 2022). Spectral features of CB-SMBHs at the final stages are determined by the accretion physics. We predict their observational appearance.

## 2 MERGING BINARIES: A CRITICAL SEPARATION

### 2.1 Fiducial numbers

In this paper, for a simplicity, we employ the third Kepler's law to approximate the orbits of merging binary SMBHs. The period is given by

$$P_{\text{orb}} = 0.1 a_2^{3/2} M_8 (1+q)^{-1/2} \text{ yr}, \quad (1)$$

where  $M_8$  is the primary SMBH mass,  $a_2 = A/10^2 R_g$  is the separation of the binary SMBHs,  $R_g = GM_\bullet/c^2$  is the gravitational radius,  $G$  is the gravitational constant,  $c$  is speed of light, and  $q$  is the mass ratio of the secondary to the primary. The orbital decay timescale due to gravitational waves is given by

$$\tau_{\text{gw}} = \frac{5}{256} \frac{c^5 A^4}{G^3 \mu M_\bullet^3} = 30.5 a_2^4 \mu^{-1} M_8 \text{ yr}, \quad (2)$$

for circle orbits from Peters (1964), where  $\mu = q(1+q)$ . The GW radiation timescale is very sensitive to the separation. The intrinsic strain amplitude is

$$h_s = 3.2 \times 10^{-17} q(1+q)^{-1/3} P_{0.1}^{-1} d_{100}^{-1} M_8^{5/3}, \quad (3)$$

with frequencies of  $\sim 10^{-6}$  Hz, where  $P_{0.1} = P_{\text{obs}}/0.1$  yr,  $d_{100} = d_L/100$  Mpc is the distances to observers in units of 100 Mpc. The GW frequency and the strain are detectable by future PTA of Square Kilometer Array (SKA) and PTA facilities. The period decays due to gravitational waves from a circle orbital binary is given by

$$\left( \frac{dP_{\text{orb}}}{dt} \right)_{\text{gw}} = -0.3 q(1+q)^{1/2} a_2^{-5/2} \text{ day yr}^{-1}, \quad (4)$$

where we make use of  $(dP_{\text{orb}}/dt)_{\text{gw}} \approx (3P/2A)(dA/dt)$ . We note that this rate in this approximation is independent of SMBH masses. Sophisticated treatment involves post-Newtonian approximations (e.g., Blanchet 2014), which is beyond the scope of this Letter. Such a decaying rate can be easily detected by monitoring campaigns.

As we show below, fates of the mini-disks around component SMBHs are determined by the orbital motion of the binaries when their separations are close enough. During the final stage, accretion onto the binaries is competing with orbital evolution governed by gravitational waves. If we can identify one target at the final stage, the periodic variabilities can be found, and period changes can be measured accurately enough for observational appearance owing to the sound instability.

### 2.2 A critical separation of binaries

It has been well understood that a cavity with a radius of  $R \approx 2A$  will be formed at the center of the circumbinary disk (CBD) after the pioneering work of Artymowicz & Lubow (1994). Many numerical simulations have been done for the configurations of accretion onto binary SMBHs. Some results from numerous simulations are well established, in particular, 3D-GRMHD simulations showed the mini-disks around the component SMBHs exist inside the cavity, and they could have different accretion rates (Farris et al. 2011; Noble et al. 2012; Giacomazzo et al. 2012; Gold et al. 2014; Zilhaõ et al. 2015; Bowen et al. 2018, 2019; Armengol et al. 2021; Cattorini et al. 2021; Combi et al. 2021; Noble et al. 2021; Paschalidis et al. 2021; Gutiérrez et al. 2022). Ultraviolet deficit appears as the major features of spectral energy distributions of the binaries (e.g., Gültekin & Miller 2012; Sesana et al. 2012; Gutiérrez et al. 2022), however,

this well-known feature remains highly uncertain in observations because of its uniqueness (dusty reddening and extinction can easily lead to a deficit similar to this effect, see [Leighly et al. 2016](#)).

In order to conveniently discuss fates of the mini-disks, we define dimensionless accretion rates of the CBD as  $\mathcal{M} = \dot{M}_{\text{CBD}}/\dot{M}_{\text{Edd}}$  from the mass rates of  $\dot{M}_{\text{CDB}}$ , where  $\dot{M}_{\text{Edd}} = L_{\text{Edd}}/c^2$  and  $L_{\text{Edd}}$  is the Eddington luminosity for each component of binary SMBHs. Component SMBHs are accreting gas supplied by the CBD, and the primary has a rate  $\dot{M}_\bullet = f_p \dot{M}_{\text{CDB}}$ , where  $f_p$  is a fraction of the CBD rates. We use  $\dot{m} = \dot{M}_\bullet/\dot{M}_{\text{Edd}}$  as the dimensional rates of the mini-disk around the primary SMBH. The properties of the mini-disks as a key to examine the observational features are insufficiently understood though there are some simplified discussions in the scheme of standard accretion disk model (e.g., [Haiman et al. 2009](#)).

### 2.2.1 Mini-disks of SMBHs

Outer radii of mini-disks are constrained by their Roche lobes,  $R_{\text{out}}/A \approx 0.49q^{2/3} / \left[ 0.6q^{2/3} + \ln(1+q^{1/3}) \right]$  (e.g., [Eggleton 1983](#)). In light of  $\mathcal{M}$ , we discuss the following cases for mini-disks of accretion onto component SMBHs. Within  $R_{\text{out}}$ , the disks are mainly governed by the single component SMBH whereas gas beyond  $R_{\text{out}}$  spread into the cavity. Gas supply to the component SMBHs is mainly determined by the interaction between the binary and the CDB, the factor  $f_p$  is beyond discussions in this paper.

*Case A:* CBDs have rates of  $\mathcal{M} \lesssim \mathcal{M}_c \approx 0.25 \alpha_{0.3}^2$  (see Eqn. 52 in [Mahadevan 1997](#)), where  $\alpha_{0.3} = \alpha/0.3$  is the viscosity parameter in advection-dominated accretion flows (ADAFs) ([Narayan & Yi 1994](#)). The entire system is in ADAF regime, which is characterized by hot temperature (close to virial ones) and inefficient radiation. The outer boundary of the ADAFs is determined by the evaporation-driven truncated radius (see Case B for a brief introduction of evaporation). [Meyer & Meyer-Hofmeister \(2002\)](#) and [Czerny et al. \(2004\)](#) approximated the truncated radius of  $r_{\text{ADAF}}^{\text{out}} = r_{\text{evap}} \approx 378.6 \mathcal{M}_{0.1}^{-0.85} \beta_{0.5}^{2.5}$  in units of  $R_g$  whereas  $r \geq r_{\text{ADAF}}^{\text{out}}$  disks follow solution of middle regions of the [Shakura & Sunyaev \(1973\)](#). As we shown in Case B,  $r_{\text{ADAF}}^{\text{out}} \gtrsim a_{\text{crit}}$  implies that evaporation dominates over the sound instability and the cavity is naturally full of hot gas.

Sound speed of ADAFs is faster than (or comparable to) the orbital motion of binary SMBHs, and hence ADAFs follow the SMBHs. Spectral energy distributions of ADAFs have been well understood. They are composed of several bumps from radio to hard X-rays due to synchrotron and multiple inverse Compton scatterings, respectively (e.g., [Manmoto 2000](#)). Figure 2 shows SEDs of ADAFs around SMBHs.

AGNs with low accretion rates usually appear as low-ionization nuclear emission-line regions (LINERs) (e.g., [Ho 2008](#)). If one LINER contains merging binary of SMBHs, as we show in §4.2, radio and X-ray emissions from the binary ADAFs show periodic variations due to Doppler boosting. Periodicity of radio and X-ray light curves will be reliable diagnostic of merging binary SMBHs. On the other hand, the transition regions from Shakura-Sunyaev disk to ADAF could radiate some UV photons (see SEDs in [Liu & Qiao 2020](#)), which are photonizing the CBDs, emerging as weak broad-line emitters.

Moreover, binary SMBHs, if existing in weak galactic nuclei, will show periodic variations in radio bands from binary ADAFs. SMBHs in normal galaxies are known to undergo Bondi accretion from the interstellar medium (ISM) evidenced by radio emissions ([Franceschini et al. 1998](#); [Nyland et al. 2016](#); [Grossová et al. 2022](#)) and X-rays of *Chandra* observations (e.g.,  $\mathcal{M} \sim 10^{-2}$  in NGC 6166 from [Di](#)

[Matteo et al. 2001](#); [Grossová et al. 2022](#)). Radio and X-ray monitoring campaigns for periodic variations will provide a robust way of identifying binary SMBHs in normal galaxies. Candidates can be selected from galaxies either with merger signatures (tails), or with mass deficit in nuclear density profiles (e.g., [Ebisuzaki et al. 1991](#)). These targets are suggested to the project of the Karl G. Jansky Very Large Array Sky Survey (VLASS) ([Lacy et al. 2020](#)), which is designed for time domain survey of radio sources. X-ray monitoring campaigns will also be useful to explore periodicity due to binary SMBHs since X-rays are less contaminated by stars in host (see the review of hot gas in normal galaxies by [Mathews & Brighenti 2003](#)).

*Case B:* CBDs have intermediate  $\mathcal{M}$  in the regime of the standard accretion disk ([Shakura & Sunyaev 1973](#)). Fates of the mini-disks depend on their radial structures. The classical model in this regime has three distinct regions: 1) inner region with a radius of  $r \leq r_{\text{inn}} = 167.1 (\alpha_{0.1} M_8)^{2/21} \dot{m}^{16/21}$  dominated by radiation pressure and electron scattering, where  $\alpha_{0.1} = \alpha/0.1$ ; 2) middle region with a radius of  $r_{\text{inn}} \leq r \leq r_{\text{mid}} = 2.5 \times 10^3 \dot{m}^{2/3}$  dominated by gas pressure and electron scattering and 3) outer regions ( $r \geq r_{\text{mid}}$ ) dominated by gas pressure and absorption (free-free, free-bound and bound-bound) (see extensive discussions in [Kato et al. 2008](#)). In this regime, the viscosity parameter  $\alpha$  is significantly smaller than that in ADAFs (e.g., [Mahadevan 1997](#)). The inner part releases most of gravitational energy, however, it turns out that the model of this part should be revised by considering more sophisticated physics.

Hot corona above the cold disk generally exists evidenced by X-ray emissions in AGNs (e.g., [Haardt & Maraschi 1991](#)). It plays a key role in the radial structure of the cold disk through very efficient evaporation (e.g., [Meyer & Meyer-Hofmeister 1994](#); [Liu et al. 1999](#)). In such a scenario, the inner part becomes ADAF, where gas pressure dominates over the radiation. Evaporation of the cold part depends on viscosity, magnetic fields and Coulomb coupling between electrons and protons in the hot corona (see a recent review of [Liu & Qiao 2020](#)). Considering the roles of magnetic fields on the suppression of evaporation, [Meyer & Meyer-Hofmeister \(2002\)](#) made numerical calculations and [Czerny et al. \(2004\)](#) obtained an approximate expression of evaporation rates in units of  $\dot{M}_{\text{Edd}}$

$$\dot{m}_{\text{evap}} = 7.1 \beta_{0.5}^{2.94} r_1^{-1.17}, \quad (5)$$

converted from the truncated radius ( $R_{\text{tr}}$ ) given by Eqn.(10) in [Czerny et al. \(2004\)](#), where  $\beta_{0.5} = \beta/0.5$  and  $\beta$  is the ratio of gas pressure to the total of gas and magnetic fields. Evaporation depends on magnetic fields because the thermal conduction coefficient can be significantly suppressed by the fields.  $\beta = 0.5$  implies a magnetic field in equipartition with the thermal gas in hot corona. The evaporation timescale is given by

$$\tau_{\text{evap}} = \frac{\pi R^2 \Sigma}{\dot{m}_{\text{evap}}} \approx 0.23 (\alpha_{0.1} \dot{m})^{-1} \beta_{0.5}^{-2.94} M_8 r_1^{4.67} f^{-1} \text{ yr}, \quad (6)$$

where  $\Sigma$  is the surface density taken from Eqn.(A3),  $f = 1 - (r_{\text{in}}/r)^{1/2}$  is the inner boundary factor and  $r_{\text{in}}$  is the inner radius of accretion disks. It should be noted that  $\tau_{\text{evap}}$  is very sensitive to radius. This timescale is comparable with orbital periods of merging binary SMBHs (see Eqn. 1).

In the inner region, the sound propagation of the mini-disks along  $r$ -direction is given by  $\tau_{\text{sound}} = R/c_s$ , where  $c_s \approx (P_{\text{rad}}/\rho)^{1/2}$  is sound speed, the radiation pressure of  $P_{\text{rad}} = aT_c^4/3$  dominates over gas pressure, where  $a$  is the black body constant and  $T_c$  is the temperature of the mid-plane (given in Appendix). For a simplicity, we still use the solution of [Shakura & Sunyaev \(1973\)](#) model for regions beyond  $R_{\text{tr}}$ , we have

$$\tau_{\text{sound}} = 0.058 \dot{m}^{-1} M_8 r_1^{5/2} f_{0.23}^{-1} \text{ yr}, \quad (7)$$

where  $c_s = 8.3 \times 10^7 \dot{m} r_1^{-3/2} f_{0.23} \text{ cm s}^{-1}$  in the inner region,  $r_{\text{in}} = 6$  is the last stable radius of the mini-disks for Schwarzschild black holes,  $f_{0.23} = f/0.23$  at  $r = 10$ . The inner part of the standard accretion disk model is divided into two parts: 1) an ADAF in the innermost region within  $R_{\text{tr}}$  and 2) a truncated cold part beyond  $R_{\text{tr}}$ . We note that the viscosity timescale  $\tau_{\text{vis}} \approx R/\nu_r = 15.5 \alpha_{0.1}^{-1} \dot{M}^{-2} r_1^{7/2} f_{0.23}^{-2} \text{ yr}$ , which is much longer than  $\tau_{\text{sound}}$  and  $P_{\text{orb}}$ , but comparable with  $\tau_{\text{gw}}$ .

*Case C:* CBDs have super-Eddington accretion rates with  $\dot{M} \gg 1$  and the mini-disks hence have  $\dot{m} \gg 1$ , which is characterized by photon trapping and transonic radial motion (Abramowicz et al. 1988; Czerny 2019). Indeed, they exist in the Universe from reverberation mapping campaigns of super-Eddington accreting massive black holes (SEAMBHs) selected from AGNs with strong optical Fe II and [O III] lines (Du et al. 2014, 2015, 2018; Du & Wang 2019). The highest  $\dot{M}$  detected so far is close to  $\sim 10^3$  from the SEAMBHs project (Du et al. 2018; Du & Wang 2019). If the CBDs have super-Eddington rates, mini-disks are expected to share a super-Eddington rate ( $f_p \lesssim 1$ ). As accretion rates increase, the mini-disks are insufficiently evaporated by the hot corona, and the evaporation radius is about  $R_{\text{tr}} \sim 6 \alpha_{0.1}^4 (\dot{m}/10^2)^2$  (see Eqn.8 in Czerny et al. 2004) approaching to the last stable orbit. ADAF disappears in super-Eddington cases evidenced by weak corona in high Eddington AGNs (e.g., Wang et al. 2004). We use the self-similar solution of super-Eddington accretion flows from Wang & Zhou (1999), and have

$$\tau_{\text{sound}} \approx 1.1 \times 10^{-3} M_8 r_1^{3/2} \text{ yr}. \quad (8)$$

In the super-Eddington cases, the sound timescale is much shorter than that in sub-Eddington accretions.

In the context of binary SMBHs, there are three competing processes governing mini-disks characterized by: 1) evaporation controlled by hot corona; 2) rapid rotation (and evolution) of orbital motion and 3) sound propagation determining the radial recovery after a perturbation. The fates of the mini-disks are controlled by the competitions among the timescales, in particular, the presence of binary SMBHs will modify accretion onto component SMBHs resulting in different features from that of a single SMBH.

### 2.2.2 Sound instability

When rotation of the binary SMBHs is fast enough (namely separations are close enough), a new instability arises depending on the competition of the orbital motion with the sound propagation (the cold part which has not been evaporated yet) and the evaporation. If both  $\tau_{\text{evap}}$  and  $\tau_{\text{sound}}$  are longer than  $P_{\text{orb}}$ , configuration of the mini-disks will be destroyed and evaporation of the disturbed disk be quenched. From  $\tau_{\text{evap}} = P_{\text{orb}}$ , we have the evaporating radius within one orbital period,

$$r_{\text{evap}} = 11.5 (\alpha_{0.1} \dot{m})^{0.21} \beta_{0.5}^{0.63} a_2^{0.32} (1+q)^{-0.11} f_{0.23}^{-0.21}. \quad (9)$$

In principle, we should solve the non-linear equation for  $r_{\text{evap}}$  because of the factor  $f$ . It turns out that  $r_{\text{evap}} \approx 11.5$  is a good approximate solution of Eqn.(9) and  $f_{0.23} \approx 1$ .

Moreover, when the sound timescale  $\tau_{\text{sound}}$  at  $r_{\text{evap}}$  is shorter than the orbital period  $P_{\text{orb}}$ , the un-evaporated part of the inner region is suffering from the sound instability. In such a case, if a radial perturbation happens, for example, tidal interaction with its companion SMBH, the mini-disks will be highly twisted so that the disks will be completely deformed and cannot recover within

one orbital period, destroying the disk configuration of accretion<sup>1</sup>. This is a new kind of instability, and is denoted as sound instability. In the meanwhile, evaporation is not able to proceed outward even for stationary hot corona. With help of Eqn. (9), we have a critical separation from  $\tau_{\text{sound}} = P_{\text{orb}}$ ,

$$a_{\text{crit}} = 75.4 \alpha_{0.1}^{0.76} \beta_{0.5}^{2.25} \dot{m}^{-0.66} (1+q)^{0.33} f_{0.23}^{2.19}, \quad (10)$$

where  $a_{\text{crit}} = A_{\text{crit}}/R_g$ .

Detailed processes of the sound instability are highly non-linear. However the instability can not be suppressed once it is triggered. For example, the Coriolis force will efficiently stretched the mini-disk along the  $\phi$ -direction. Moreover, the contraction of the binary separations will increase with orbital evolution and the  $r$ - perturbation holds until merger. It is interesting to note that this critical separation is independent of SMBH mass, but mildly dependent of accretion rates and sensitive to the magnetic fields. For  $q \sim 1$ , we have  $a_{\text{crit}} \approx 95$ . CB-SMBHs with separations less than  $a_{\text{crit}}$  are not allowed to have their own mini-disks. This new kind of instability purely arises from the competition between the orbital motion and sound propagation. Without cold mini-disks, the binary SMBHs will radiate peculiar form of spectral energy distributions.

As to Case A and C, the sound instability is suppressed. Comparing  $P_{\text{orb}}$  with sound timescales of super-Eddington accretion, we find that it is always longer than  $\tau_{\text{sound}}$  (even for  $r \sim a$ ), and super-Eddington is stable under the orbital motion. It is then expected that SEDs from super-Eddington accretion known as  $F_\nu \propto \nu^{-1}$  holds (Wang & Zhou 1999; Wang et al. 1999) in the merging binary SMBHs. Component SMBHs of the merging binaries with super-Eddington accretion rates share one common broad-line region (BLR). They should show spectral features of strong optical Fe II and weak [O III] lines in super-Eddington accreting AGNs (Du & Wang 2019).

In a summary, mini-disks around each SMBH are undergoing the sound instability due to the fact that orbital motion is faster than the sound propagation when the binary separations are close enough. The mini-disks cannot exist due to the instability unless it has highly super-Eddington rates. The sound instability drives a conversion of cold mini-disks into hot gas following the orbital motion.

We would like to point out validity of the present discussions. Corrections of timescales in the co-moving frame of the fluid orbiting the mini-disks can be neglected since it is at a level of  $O(10^{-2})$  for a region beyond  $\sim 10^2 R_g$ . We note that this can be justified by the pseudo-Newtonian potential of  $\Psi = -GM_*/(R - 2R_g)$  by Paczyński & Wiita (1980). We note that magnetic field might stabilize the mini-disks when the fields are strong enough as shown in numerical simulations (Cattorini et al. 2022). The sound instability discussed in this paper could be weakened. The issues of mini-disks are highly non-linear and detailed analysis should be done from dynamical equations.

## 3 ACCRETION ONTO BINARIES OF SMBHS

### 3.1 Bondi accretion

Gas remains in the cavity, and its density and temperature are determined by the energy supplied by the rotation energy of the binary. The orbital velocity of the primary SMBH with respect to the

<sup>1</sup> Accretion flows can be transonic at some radii of a few  $R_g$  (Muchotrzeb & Paczyński 1982; Abramowicz et al. 1988), but the radii are much smaller than the evaporation radius. The transonic effects can be neglected in the sound instability.

mass center is  $v_{\bullet}/c = q(1+q)^{-1/2}a^{-1/2}$ , which is much faster than the disk sound speed. Shocks formed by the fast orbital motion with a Mach number of  $\mathcal{M} \sim v_{\bullet}/c_s \sim 10^3$  will efficiently heat the cavity gas. SMBHs gravitationally bound more gas at earlier stage of the interaction when the gas is not hot so that SMBHs have very large cross section colliding with cavity gas. Heating details are complicated, but the temperature is expected to be close to the virial temperature, namely,  $T \sim m_p c^2 / kr \approx 1.1 \times 10^{11} r_2^{-1}$  K. In such a hot plasma, the Coulomb coupling between proton and electrons are so inefficient that electron temperatures are much lower than that of protons (Stepney & Guibert 1983). Electrons keep temperatures  $\sim 10^9$  K (e.g., Shapiro et al. 1976; Rees et al. 1982) and Eqn. 40 (in Mahadevan 1997). We take  $T = 10^9 T_9$  K in this paper. Cavity gas is cooling through free-free emission with a timescale

$$\tau_{\text{ff}} = 5.7 \times 10^3 T^{1/2} n_e^{-1} \text{ yr}, \quad (11)$$

where  $n_e$  is the number density of electrons in the cavity, and  $T$  is the temperature of cavity gas. The cooling should be balanced by heating due to rotation of the binary, this implies  $\tau_{\text{ff}} = \tau_{\text{gw}}$ , we have

$$n_e = 6.0 \times 10^6 T_9^{1/2} a_2^{-4} \mu M_8^{-1} \text{ cm}^{-3}. \quad (12)$$

SMBHs cannot have their own mini-disks with accretion rates of the standard model, however, they are still accreting in Bondi mode with a rate of (e.g., Kato et al. 2008)

$$\dot{M}_{\text{Bon}} = \frac{4\pi G^2 M_{\bullet}^2 n_e m_p}{(c_s^2 + v_{\bullet}^2)^{3/2}} \approx \frac{4\pi G^2 M_{\bullet}^2 n_e m_p}{v_{\bullet}^3}, \quad (13)$$

in the cavity context, where  $m_p$  is the proton mass. The sound speed of the cavity is poorly known, but it cannot exceed the orbital velocity. Given the cavity density, we have dimensionless accretion rates of  $\mathcal{M}_{\text{Bon}} = \dot{M}_{\text{Bon}} / \dot{M}_{\text{Edd}}$

$$\mathcal{M}_{\text{Bon}} = 0.1 q^{-3} (1+q)^{3/2} a_2^{3/2} n_7 M_8, \quad (14)$$

where  $n_7 = n_e / 10^7 \text{ cm}^{-3}$ . It should be noted that Eqn. (14) is only valid for the primary when  $v_{\bullet} \gg c_s$ .

We estimate the electron density of the hot cavity from balance between cooling and heating. Cavity gas is partially from evaporation and also from the twisted mini-disks. The Bondi spheres of component SMBHs greatly enhance the efficiency of heating gas in the cavity, but also significantly affects gas supply from the CBD. Detailed transition of mini-disks into hot gas is of great interests as to AGN variabilities, and should be investigated by numerical simulations.

### 3.2 Circumbinary disk

A cavity of accretion disk will be formed through the tidal torque of the binary with accretion disk. We approximate the binary SMBHs as a single one in the circumbinary disk (CBD), the effective temperature is

$$T_{\text{eff}} = \left( \frac{3GM_{\bullet}\dot{M}}{8\pi\sigma_{\text{SB}}R^3} \right)^{1/4} = 1.9 \times 10^4 (\mathcal{M}/M_8)^{1/4} r_2^{-3/4} \text{ K}, \quad (15)$$

where  $r_2 = R/10^2 R_g$  is the radius of the CBD to the mass center of the binary, and the boundary factor  $f \approx 1$  at  $r = 10^2$ . The CBD is radiating photons with energies of

$$\epsilon_{\text{CBD}} \approx 4.5 (\mathcal{M}/M_8)^{1/4} r_2^{-3/4} \text{ eV}, \quad (16)$$

which is significantly lower than the ionization energy of hydrogen ( $\epsilon_{\text{H}} = 13.6 \text{ eV}$ ) and first level of magnesium atoms ( $\epsilon_{\text{Mg}^+} = 7.6 \text{ eV}$ ).

In this paper, we focus on the case of binary SMBHs with separations less than  $A_{\text{crit}}$ . The two SMBHs share a common broad-line region (BLR), and hence the BLR follows the well-known  $R - L$  relation (Kaspi et al. 2000; Bentz et al. 2013; Du & Wang 2019). For a CBD with  $\mathcal{M} \sim 1$ , Eqn. (16) indicates the lack of ionizing photons in BLR. The merging binaries of SMBHs are expected to not have significant emission lines such as Balmer lines and Mg  $\pi\lambda 2798\text{\AA}$  though they have normal optical continuum as AGNs. However, Mg  $\pi$  line appears when  $\mathcal{M} \gtrsim 9$  (slightly super-Eddington; see Du & Wang 2019) but it could be weak. When  $\mathcal{M} \gtrsim 90$ , Balmer lines just appear and Mg  $\pi$  line could be normal, but high ionization line C IV  $\lambda 1549\text{\AA}$  ( $\epsilon_{\text{C}^{3+}} = 47.9 \text{ eV}$ ) will never appears unless  $\mathcal{M} \gtrsim 10^4$  much exceeding the known accretion rates of SEAMBHs (Du & Wang 2019). Generally, these merging binaries appear as optically bright nuclei without strong broad emission lines.

## 4 OBSERVATIONAL SIGNATURES

### 4.1 SEDs

Emergent spectra of the merging binaries are composed of two parts: 1) ADAF emissions from the primary and secondary SMBHs and 2) CBD emissions. Emissions from the cavity can be neglected if compared with Bondi accretion<sup>2</sup>. We apply the ADAF model to merging SMBHs for their emergent spectra formulated by Manmoto (2000) (see also Li et al. 2009). Bolometric luminosity of ADAFs is about  $L_{\text{ADAF}} \approx 3.0 \times 10^{43} \alpha_{0.3}^{-2} M_8 \mathcal{M}_{0.1}^2 \text{ erg s}^{-1} \propto \mathcal{M}^2$  (see Eqn. 49 in Mahadevan 1997), where  $\mathcal{M}_{0.1} = \mathcal{M}/0.1$ . Figure 2 shows the characteristic emergent spectra. Emissions from the SMBH Bondi accretion span from radio to X-rays, but its powers are significantly lower than the CBD. For one target at a distance of 100 Mpc, radio fluxes received by the observers are about  $F_{100\text{GHz}} \approx 2.6 \mu\text{Jy}$  at  $\nu = 100\text{GHz}$ , which is significantly higher than sensitivity of SKA ( $0.1 \mu\text{Jy}$ ), but much lower than the current VLA sensitivity. In the meanwhile, we also mark the detectable level of sensitivity of X-ray missions for future detections (*Chandra*, *NuSTAR*, *XMM-Newton* and *Swift*) at 100 Mpc. It is clear that the current missions are able to detect the periodic variations. Some weak-line quasars have similar SEDs to the predicted shape in Wu et al. (2012) and Luo et al. (2015) samples (*GALEX* data were used) and X-shooter sample (Plotkin et al. 2015), but the UV deficit should be necessarily investigated by more observations. Moreover, Doppler boosting can be tested with the multiwavelength continuum.

Since optical emissions are from the CBD in standard regime, it is expected that radio emissions are much fainter than optical and they will show radio-weak or radio-quiet properties. Comparing with optical emissions, X-rays are much fainter showing X-ray weak. Radio emissions depend on the outer boundary radius, where we take it to be  $50R_g$ . Future detection at  $\sim 10 - 100 \text{ GHz}$  will reveal the radio periodical variations if merging binaries exist.

For super-Eddington accretion onto each components of the binaries, its optical to UV continuum are characterized by the known spectra of  $L_{\nu} \propto \nu^{-1}$ . This results from the effective temperature distribution of  $T_{\text{eff}} \propto r^{-1/2}$  due to photon trapping effects (Wang & Zhou 1999; Wang et al. 1999).

<sup>2</sup> According to self-similar solution of ADAF (see their Eq. 12.5 in Narayan & Yi 1995), we have ADAF gas density of  $\sim 10^8 \text{ cm}^{-3}$  at  $r = 10^2$  for  $\mathcal{M} = 0.1$ . Since the cavity density of hot gas is about 3% of the ADAF, cavity gas emission is only of  $\sim 10^{-3}$  of the ADAF from free-free emissions of hot plasma.

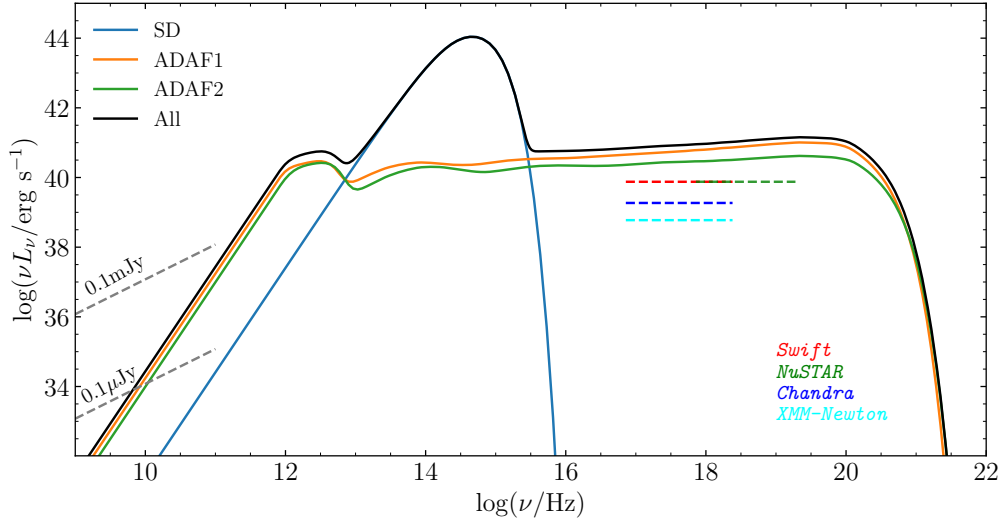


**Figure 2.** Characterized shapes of spectral energy distributions of the binary system: 1) two-ADAF emissions: yellow line for  $(M_{\bullet}/M_{\odot}, \dot{M}) = (10^8, 0.1)$  and green for  $(10^7, 0.07)$ ; and 2) CDB emissions (blue line for  $\dot{M} = 1$ ) from standard disk (SD). We assume that SMBHs are Schwarzschild black holes, outer and inner boundary radii are  $(50, 6) R_g$ . Radio emissions from ADAFs are expected to undergo periodic variabilities. Optical emissions are similar to normal AGNs, but they are radio-quiet and X-rays are weak. Detection levels of observations from radio to X-rays are marked, showing feasible detections in X-rays.

SEDs of periodical AGNs and quasars (Graham et al. 2015a; Charisi et al. 2016; Liu et al. 2019) from radio to UV (GALEX data) are found to be similar to that of normal AGNs and quasars, and the periodicity of the sample identified from  $\geq 1.5$  cycle light curves may be false positive (Guo et al. 2020). On the other hand, periodicity of AGNs and quasars is needed to be confirmed with longer baselines.

## 4.2 Doppler boosting

D’Orazio et al. (2015) suggested that orbital motion of binary SMBHs causes periodical variations due to Doppler boosting effects if the separations are small enough. Supposing that the orbital plane ( $XOY$ ) has an inclination angle of  $i_o$  with respect to observer’s line of sight (in  $XOZ$  plane), the direction of observers is  $\vec{n}_o = (\sin i_o, 0, \cos i_o)$  and the SMBH are  $\vec{n}_{\bullet} = (\cos \phi, \sin \phi, 0)$ , where  $\phi = 2\pi t/P_{\text{orb}}$  is the phase angle. The angle between SMBH motion direction and the observers is given by  $\cos \theta = \vec{n}_o \cdot \vec{n}_{\bullet} = \sin i_o \cos \phi$ . The Doppler factor is given by

$$\mathcal{D} = \frac{1}{\gamma(1 - \beta \cos \theta)}, \quad (17)$$

where  $\gamma = 1/\sqrt{1 - \beta^2}$  is the Lorentzian factor of SMBHs and  $\beta$  is the velocity in units of light speed. Considering the invariance of  $F_{\nu}/\nu^3$ , we have the total fluxes from the two SMBHs

$$F_{\text{tot}} = \sum_{i=1}^2 \frac{F_i}{[\gamma_i(1 - \beta_i \cos \theta_i)]^{3-\alpha_{\nu}}}, \quad (18)$$

where  $F_i$  is the spectral flux from the  $i$ -th ADAF,  $\beta_1 = q(1+q)^{-1/2}a^{-1/2}$  and  $\beta_2 = (1+q)^{-1/2}a^{-1/2}$  are velocities of the primary and the secondary SMBHs around the binary mass center, respectively, their projected angles are  $\cos \theta_1 = \sin i_o \cos(2\pi t/P_{\text{orb}})$  and  $\cos \theta_2 = \sin i_o \cos(2\pi t/P_{\text{orb}} + \pi)$ , and  $\alpha_{\nu}$  is the spectral index of ADAFs. Path differences of photons from the primary and the secondary SMBHs are neglected since  $A/c \ll P_{\text{orb}}$ .

According to the scaling law of radio luminosity  $L_{\text{rad}} \propto \dot{M}^{3/2}$

from ADAFs (see Eqn. 24 in Mahadevan 1997), we have  $F_1 \propto q^{-9/2}(1+q)^{3/4}$  and  $F_2 \propto q^{11/2}(1+q^{-1})^{3/4}$ . For radio spectra of ADAFs, we take  $\alpha_{\nu} \approx 1.5$  in our calculations. Radio fluxes from ADAFs are very sensitive to mass ratios due to the Bondi accretion as well as inclination angle. In Figure 3, we show the periodic light curves of ADAF radio emissions. It is expected that X-rays should have the same periods with radio, but variation amplitudes are different from radio because of different spectral indices from radio bands.

## 4.3 Warped disks

Radio emissions should be periodic, and optical emissions are also periodic if the CBD is warped with a tilt angle ( $\beta_t$ ). The processing CBD will show periodic variations due to emitting area varying with time projected to observers (e.g., Martin et al. 2007), namely, we are receiving photons from periodically-changing surface of the warped disk. The CBD precession driven by tidal torque of the binary with a circular orbit will show a modulations of received fluxes with a period given by Hayasaki et al. (2015)

$$\tau_{\text{pre}} = \frac{4(1+q)^2}{3\pi q \cos \beta_t} \left(\frac{R}{A}\right)^{7/2} P_{\text{orb}} \approx 19.2 P_{\text{orb}}, \quad (19)$$

for  $\cos \beta_t = 0.5$  and  $q = 1$ , where we take  $R/A = 2$ . This implies that the optical periods are ten times the radio periods. Target selections of radio periodic AGNs could be favored from those with optical periods of a few years.

## 4.4 Period changes

Period changes due to GW (see Eqn.4) can be exactly measured by radio and X-ray campaigns as well as X-ray light curves. How to measure the orbital parameters of the merging binary SMBHs is a challenging task. Fortunately, SARM can accurately measure the total mass of binary SMBHs with the weak lines, like for 3C 273 (the best measurements with accuracy of about 15% in Wang et al. 2020;

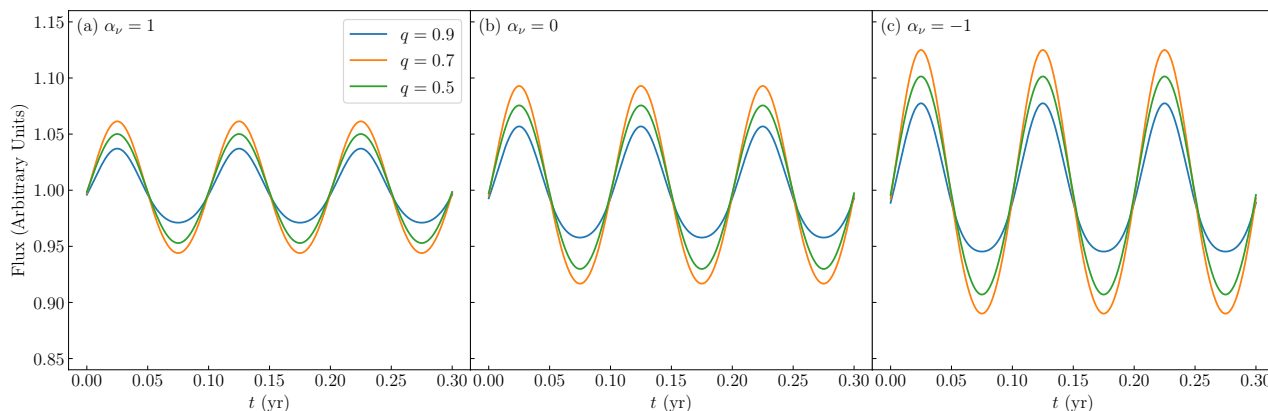


**Figure 3.** Radio light curves of binary SMBHs with ADAF emissions modulated by Doppler boosting. We take the primary SMBH of  $M_{\bullet} = 10^8 M_{\odot}$ , and a period of 0.1 yr. An inclination angle of  $30^{\circ}$  is assumed. Here we plot three indexes for different bands: 1) cm band ( $\alpha_{\nu} \approx 1$ ); 2) mm band ( $\alpha_{\nu} \approx 0$ ) and 3) sub-millimeter ( $\alpha_{\nu} \approx -1$ ). Though the periods of different bands are same but the amplitudes are dependent of wavelengths. If X-ray light curves are obtained through monitoring campaigns, the dependence of Doppler boosting on wavelength can be tested.

Li et al. 2022). With orbital parameters, we can estimate the expected period changes and compare them with observations ( $\sim 0.3 \text{ day yr}^{-1}$ ) from Eqn. (4) provided radio periods are accurately measured. Such a test is feasible for the merging binary SMBHs. This way is exactly same with that of Hulse & Taylor (1975) for binary pulsars in radio. Moreover, if future PTA becomes efficient enough to test individual merging binary SMBHs, low frequency GW can be observationally tested for gravity theory.

#### 4.5 Relativistic jets

As one of well-known properties, relativistic jets/outflows can be naturally produced from ADAFs of SMBHs (Narayan & Yi 1994; Blandford et al. 2019). It is thus to expect jets/outflows from SMBHs inside the hot cavity. The jet powers from extreme Kerr SMBHs can be simply estimated by  $L_{\text{jet}} \approx \eta_{\text{BZ}} \dot{M} c^2 = 2.8 \times 10^{43} \eta_{0.02} \dot{M}_{0.1} M_8 \text{ erg s}^{-1}$  (Armitage & Natarajan 1999), where  $\eta_{0.02} = \eta_{\text{BZ}}/0.02$  is the radiative efficiency of the Blandford-Znajek (BZ) mechanism. This BZ process is much more efficient than ADAF emissions ( $L_{\text{ADAF}} \ll L_{\text{jet}}$ ) if  $\dot{M} \ll 0.1$ .

If the component SMBHs (extreme Kerr ones) are generating their own jets independently, double two-pair jets will be produced from the binary SMBH system (e.g. Paschalidis et al. 2021), even there is the third jet produced by pumping rotating energy after the binary SMBHs merge. In the presence of relativistic jets, observers receive two kinds of radio components: 1) binary ADAFs and 2) double two-pair jets. Even the jets are misaligned to the observers, radio emissions are still quite strong as shown by  $L_{\text{jet}}$ . The light curves will be complicated and depend on orientations of jets ( $\Theta_0$ ) and their Lorentzian factor ( $\Gamma$ ). The observed luminosity from the jets is  $L_{\text{obs},\nu} = \mathcal{D}_{\text{jet}}^{3-\alpha_{\nu}} L_{\text{jet},\nu}$ , where  $\mathcal{D}_{\text{jet}}$  is the Doppler factor, and  $\mathcal{D}_{\text{jet}} \sim 10$  is common for jets but depends on  $\Theta_0$ . Jet's apparent luminosity is much brighter than ADAF itself. When jets are spiraling outward, and the relativistic Doppler factor is function of time, showing periodic variations. This is similar to the jet case in SS 433 (Hjellming & Johnston 1981), whose periodic variations are caused by orbital and precession of jets. We will separately discuss this issue in a future paper.

## 5 SEARCHING FOR MERGING BINARIES

Merging binary SMBHs are characterized by several features: 1) weak broad emission lines (Mg II and H $\beta$ ); 2) continuum with UV deficit (unless those candidates with super-Eddington rates); 3) plausibly periodic variations in radio, optical and X-ray bands, but the two periods could be very different.

It remains open to estimate SMBH masses as a big issue of estimating separations of SMBH binaries. Generally SMBH masses can be estimated by Magorrian relation or  $M_{\bullet} - \sigma$  relation for radio galaxies or weakly active galactic nuclei (e.g., Kormendy & Ho 2013). If the hosts of SMBH binaries are normal AGNs, we can employ the technique of reverberation mapping not only for SMBH mass but also orbital parameters including ellipticity, mass ratios and semi-major axis (Wang et al. 2018; Songsheng et al. 2020; Kovačević et al. 2020b). This needs high spectral resolution spectrograph installed on 8m telescope (Songsheng et al. 2020). Joint analysis of GRAVITY/VLTI and RM data will be more robust for orbital parameters.

### 5.1 Weak line quasars and optical periodicity

Weak line quasars (WLQs), which are usually defined by EW(C iv) less than  $10 \text{ \AA}$ , have been discovered by SDSS (Fan et al. 1999, 2006; Anderson et al. 2001; Collinge et al. 2005; Diamond-Stanic et al. 2009), however, nature of their multiple SEDs remains open so far (Wu et al. 2012; Plotkin et al. 2015; Luo et al. 2015; Ni et al. 2022). They are either radio-quiet or radio-loud (Plotkin et al. 2010), and about half of WLQs are X-ray weak (Luo et al. 2015; Ni et al. 2022), however, the UV continuum is uncertain somehow. Some WLQs seem to have SEDs similar to our prediction in this work (see X-shooter spectrum in some WLQs in Plotkin et al. 2015). It will be interesting to test if these WLQs have periodic variations at optical bands.

Guo et al. (2019) investigate UV continuum of Graham et al. (2015a) sample to check their UV deficit, however, they have not found this deficit from this sample. On the other hand, UV deficit could be caused by dusty reddening/extinction, for example, Mrk 231 (Yan et al. 2015; Leighly et al. 2016). On the one hand, periodicity of Graham et al. (2015a), Charisi et al. (2016) and Liu et al. (2019) samples should be tested by extending baseline of light

curves. Dependence of Doppler boosting effects on different wavebands has been checked for some objects (Charisi et al. 2016; Chen et al. 2021). Moreover, it should be mentioned that only periodicity of optical variations is not enough to justify binary SMBHs. It is far away to draw conclusions as to binarity of SMBHs in the current sample. Large Synoptic Survey Telescope (LSST) is highly expected to show high quality light curves of AGNs to search for candidates of merging SMBHs in near future.

## 5.2 Radio periodic AGNs

To search for the binaries, we should monitor AGNs for periodicity. Time-domain survey of VLASS has been designed by Lacy et al. (2020) (PKS 2131-021 is one of the targets of VLASS). This lends opportunity of searching for radio periodic light curves of the candidates of merging binary SMBHs. With great progress of optical periodic AGNs, we should pay more attention to them in radio (also in X-rays).

We would mention the possibility that the binary ADAFs inside the cavity could produce relativistic jets. If jets are in alignment with observer's line of sight, we will see a radio-loud AGNs. King et al. (2013) reported a radio light curve with a period of 120 – 150 days in the blazar J1359+4011, which is very different from other blazars with periodical variations. This was explained by disk oscillations similar to that in X-ray binary because this period is much shorter than the known physics of jet/disk precession (King et al. 2013). Alternatively, we might explain this from the orbital Doppler boosting of merging binary SMBHs. Recently, Zhang et al. (2022) report double periods of 345 day and 386 day in NGC 1275 (3C 84), providing indirect evidence for hypothesis of close binary SMBHs. Recently, radio periodicity of PKS 2131-021 is found as a candidate of binary SMBHs (O'Neill et al. 2022).

## 5.3 Detection probabilities

Considering AGN lifetimes ( $\tau_{\text{AGN}}$ ), we may detect the merging binary SMBHs with a probability of  $p \approx \tau_{\text{gw}}/\tau_{\text{AGN}} \sim 3 \times 10^{-6}$  if  $\tau_{\text{AGN}} = 10^7$  yr is taken (which is the radial timescale of accretion flows at its outer boundary). For the current sample of million AGNs and quasars<sup>3</sup>, we may have a few cases. However, we should note that  $\tau_{\text{gw}}$  is very sensitive to the separations of binaries and  $\tau_{\text{AGN}}$  is highly uncertain. If we take  $\tau_{\text{AGN}} \sim 10^5$  yr (Schawinski et al. 2015), we have  $p \sim 3 \times 10^{-4}$  implying  $\sim 300$  AGNs as merging binary SMBHs in the Universe. This is a quite large number. Moreover, this crude estimation could be improved by including evolution of orbits.

In summary, searching for candidates from WLQs with periodical variations is feasible in radio and X-ray bands, in particular optical (ZTF and LSST). Moreover, UV deficit is explored by the X-shooter and HST UV observations which is also a key to explain nature of WLQs.

## 6 SUMMARY

Merging binary supermassive black holes are completely elusive in observations because accretion onto the binaries is insufficiently understood. In this paper, we investigate fates of the mini-disks with three regimes of accretion rates from low to super-Eddington status. In the regime of standard accretion disks, the innermost regions of the

mini-disks are evaporated through thermal conduction of hot corona, and the mini-disks are truncated. We find a new instability of the mini-disks when the binary SMBHs are close enough. In such a context, the sound propagation timescale is longer than the orbital period of the binaries so that the disks are highly twisted and destroyed. For binary SMBHs of  $\sim 10^8 M_{\odot}$  with typical orbital values, the critical separation is about  $\sim 10^2$  gravitational radius (orbital periods are about 0.1 yr). For low accretion and super-Eddington regimes, the sound instability disappears.

Heated by the orbital motion of the binaries, cavity is then full of hot gas and SMBHs are accreting through Bondi mode unless binaries with extreme super-Eddington accretion rates. Emissions from the Bondi accretion are modulated by the orbital motion and Doppler boosting effects. For radio-quiet AGNs, radio monitoring campaigns are expected to detect periodic variations at these bands. If normal galaxies contain binary SMBHs, they will show similar periodical variations, in particular, radio and X-ray campaigns of monitoring candidates are suggested because of less contaminations from host galaxies.

For binary SMBHs with intermediate accretion rates, the UV deficit as a continuum characteristic appears and AGNs thus show weak broad emission lines. The circumbinary disk is radiating in optical band whereas Bondi accretion of SMBHs in the cavity is generating multiwaveband continuum from radio to hard X-rays. Moreover, Balmer lines disappear owing to the significant lack of ultraviolet photons. However, for binaries with super-Eddington rates, spectral energy distributions keep the form of  $F_{\nu} \propto \nu^{-1}$  without UV deficit. Emission line features should be similar to those SEAMBHs (strong optical Fe II and weak [O III] lines). There is an interesting case of warped disks showing periodical variations in optical bands with periods of ten times the radio periods if the circumbinary disks are misaligned with the orbital plane.

Searching for merging binary SMBHs is very challenging since they could occupy a very tiny fraction ( $\sim 10^{-6} - 10^{-3}$ ) of the current AGN sample. Candidates of merging SMBHs are expected to show observational signatures characterized by ultraviolet deficit with/without weak emission lines as well as X-ray weak emissions (and potentially with optical periods). For extreme Kerr SMBHs in merging binaries, they will generate relativistic jets. In this case, calculations of light curves will be complicated and beyond the scope of this paper. Radio and X-ray periodic variations are the key diagnostic of the binaries, current VLA can focus on a systematic search from radio-loud AGNs and future SKA from radio-quiet ones (e.g., Bignall et al. 2015).

## ACKNOWLEDGEMENTS

JMW is grateful to L. C. Ho for interesting discussions, and to E. Qiao for evaporation processes. This research is supported by grant 2016YFA0400700 from the Ministry of Science and Technology of China, by NSFC-11991050, -11773029, -11833008, -11690024, -11721303, -11991052 -11573026, -11873048, -11703077, -11503026, and by the CAS Key Research Program (KJZDEW-M06) and by the Key Research Program of Frontier Sciences, CAS, grant QYZDJ-SSW-SLH007.

## DATA AVAILABILITY

The data underlying this article will be shared on reasonable request to the corresponding author.

<sup>3</sup> <https://heasarc.gsfc.nasa.gov/W3Browse/all/milliquas.html>



## APPENDIX A: SOLUTIONS OF STANDARD ACCRETION DISK MODELS

Mini-disks as accretion flows of component SMBHs mainly involve the inner region, where radiation pressure and scattering dominate. We employ the solutions of standard accretion disk models (Shakura & Sunyaev 1973), radial velocity, temperature, surface density, mass density given by

$$v_r = 1.4 \times 10^6 \alpha_{0.1} \dot{M}^2 r_1^{-5/2} f \text{ cm s}^{-1}, \quad (\text{A1})$$

$$T_c = 4.8 \times 10^5 (\alpha_{0.1} M_8)^{-1/4} r_1^{-3/8} \text{ K}, \quad (\text{A2})$$

$$\Sigma = 1.1 \times 10^4 (\alpha_{0.1} \dot{m})^{-1} r_1^{3/2} f^{-1} \text{ g cm}^{-2}, \quad (\text{A3})$$

and

$$\rho = 1.0 \times 10^{-10} (\alpha_{0.1} M_8)^{-1} \dot{m}^{-2} r_1^{3/2} f^{-2} \text{ g cm}^{-3}, \quad (\text{A4})$$

respectively, in the inner region (e.g., Kato et al. 2008).

## REFERENCES

- Abramowicz, M., Czerny, B., Lasota, J.-P. & Szuszkiewicz, E. 1988, *ApJ*, 332, 646
- Anderson, S. F., Fan, X., Richards, G. T., et al. 2001, *AJ*, 122, 503
- Armengol, F. G. L., Combi, L., Campanelli, M., et al. 2021, *ApJ*, 913, 16,
- Armitage, P. J. & Natarajan, P. 1999, *ApJ*, 523, L7
- Artymowicz, P., & Lubow, S. H. 1994, *ApJ*, 421, 651
- Begelman, M. C., Blandford, R. D. & Rees, M. J. 1980, *Nature*, 287, 307
- Bentz, M. C., Denney, K. D., Grier, C. J., et al. 2013, *ApJ*, 767, 149
- Bignall, H. E., Croft, S., Hovatta, T. et al. *Proceedings of Advancing Astrophysics with the Square Kilometre Array*. arXiv:1501.04627
- Blanchet, L. 2014, *Living Rev. Relativity*, 17, 2
- Blandford, R., Meier, D. & Readhead, A. 2019, *ARA&A*, 57, 467
- Bogdanovic, T., Miller, M. C. & Blecha, L. 2021, arXiv:2109.03262
- Bowen, D. B., Mewes, V., Campanelli, M., et al. 2018, *ApJ*, 853, L17
- Bowen, D. B., Mewes, V., Noble, S. C., et al. 2019, *ApJ*, 879, 76
- Brotherton, M. S., Du, Pu, Xiao, M. et al. 2020, *ApJ*, 905, 77
- Cattorini, F., Giacomazzo, B., Haardt, F., & Colpi, M. 2021, *PhRvD*, 103, 103022
- Charisi, M., Bartos, I., Haiman, Z., et al., 2016, *MNRAS*, 463, 2145
- Charisi, M., Taylor, S. R., Runnoe, J., Bogdanovic, T., & Trump, J. R. 2022, *MNRAS*, 510, 5929
- Chen, Y.-C., Liu, X., Liao, W.-T. et al. 2022, *MNRAS*, 499, 2245
- Chen, Y.-C., Liu, X., Liao, W.-T. & Guo, H. 2021, *MNRAS*, 507, 4638
- Collinge, M. J., Strauss, M. A., Hall, P. B. et al. 2005, *AJ*, 129, 2542
- Combi, L., Armengol, F. G. L., Campanelli, M. et al. 2021, *ApJ*, arXiv:2109.01307
- Cattorini, F., Maggioni, S., Giacomazzo, B. et al. 2022, *ApJ*, 930, L1
- Czerny, B. 2019, *Universe*, 5, 131
- Czerny, B., Rózańska, A., & Kuraszkiewicz, J. 2004, *A&A*, 428, 39
- Decarli, R., Dotti, M., Fumagalli, M. et al. 2013, *MNRAS*, 433, 1492
- De Rosa, A., Vignali, C., Bogdanović, T., et al. 2019, *New A Rev.*, 86, 101525
- Diamond-Stanic, A. M., Fan, X., Brandt, W. N., et al. 2009, *ApJ*, 699, 782
- Di Matteo, T., Johnstone, R. M., Allen, S. W. & Fabian, A. C. 2001, *ApJ*, 550, L19
- Doan, A., Eracleous, M., Runnoe, J. C., et al. 2020, *MNRAS*, 491, 1104
- D’Orazio, D. J., Haiman, Z., Schiminovich, D. 2015, *Nature*, 525, 351
- Dotti, M., Bonetti, M., D’Orazio, Daniel J., et al. 2022, *MNRAS*, 509, 212
- Hu, C., Lu, K.-X., et al. 2014, *ApJ*, 782, 45
- Du, P., Hu, C., Lu, K.-X., et al. 2015, *ApJ*, 806, 22
- Du, P., Brotherton, M. S., Wang, K., et al. 2018, *ApJ*, 869, 142
- Du, P. & Wang, J.-M. 2019, *ApJ*, 886, 42
- Ebisuzaki, T., Makino, J., & Okumura, S. K. 1991, *Nature*, 354, 212
- Eggleton, P. P. 1983, *ApJ*, 268, 368
- Fan, X., Strauss, M. A., Gunn, J. E., et al. 1999, *ApJ*, 526, L57
- Fan, X., Strauss, M. A., Richards, G. T., et al. 2006, *AJ*, 131, 1203
- Farris, B. D., Liu, Y. T., & Shapiro, S. L. 2011, *PhRvD*, 84, 024024
- Foord, A., Liu, X., Gültekin, K. et al. 2021, arXiv:2110:02982
- Franceschini, A., Vercellone, S. & Fabian, A. C. 1998, *MNRAS*, 297, 817
- Giacomazzo, B., Baker, J. G., Miller, M. C., Reynolds, C. S., & van Meter, J. R. 2012, *ApJ*, 752, L15
- Gold, R., Paschalidis, V., Ruiz, M., et al. 2014, *PhRvD*, 90, 104030
- Graham M. J. et al., 2015a, *Nature*, 518, 74
- Graham, M. J., Djorgovski, S. G., Stern, D. et al. 2015b, *MNRAS*, 453, 1562
- Gravity Collaboration; Abuter, R.; Accardo, M. et al. 2017, *A&A*, 602, A94 (GC2017)
- Gravity Collaboration; Sturm, E.; Dexter, J. et al. 2018, *Nature*, 563, 657 (GC2018)
- Gravity Collaboration; Amorim, A.; Bauböck, M. et al. 2020, *A&A*, 643, 154 (GC2020)
- Gravity Collaboration; Amorim, A.; Bauböck, M. et al. 2021, *A&A*, 648, 117 (GC2021)
- Grossová, R., Werner, N., Massaro, F. et al. 2022, *ApJS*, 258, 30
- Guo, H., Liu, X., Shen, Y., et al. 2019, *MNRAS*, 482, 3288
- Guo, H., Liu, X., Zafar, T. Liu, W.-T. 2020, *MNRAS*, 492, 2910
- Gültekin, K. & Miller, J. M. 2012, *ApJ*, 761, 90
- Gutiérrez, E. M., Combi, L., Noble, S. C. et al. 2022, arXiv:2112.09773
- Haardt, F. & Maraschi, L. 1991, *ApJ*, 380, L51
- Haiman, Z., Kocsis, B. & Menou, K. 2009, *ApJ*, 700, 1952
- Hayasaki, K., Sohn, B. W., Okazaki, A. T. et al. 2015, *JCAP*, 7, 5
- Hjellming, R. M. & Johnston, K. J. 1981, *ApJ*, 246, L141
- Ho, L. C. 2008, *ARA&A*, 46, 475
- Hulse, R. A. & Taylor, J. H. 1975, *ApJ*, 195, L51
- Ji, X., Lu, Y., Ge, J., Yan, C. & Zhao, S. 2021, *ApJ*, 910, 101
- Kaspi, S., Smith, P. S., Netzer, H., et al. 2000, *ApJ*, 533, 631
- Kato, S., Fukue, J. & Mineshige, S. 2008, *Black Hole Accretion*, Kyoto University Press.
- King, O. G., Hovatta, T., Max-Moerbeck, W. et al. 2013, *MNRAS*, 436, L114
- Korredny, J. & Ho, L. C., 2013, *ARA&A*, 51, 511
- Kovačević, A. B., Wang, J.-M., & Popović, L. Č. 2020, *A&A*, 635, A1
- Kovačević, A. B., Songsheng, Y.-Y., Wang, J.-M. & Popović, L. 2020, *A&A*, 644, 88
- Lacy, M.; Baum, S. A.; Chandler, C. J. et al. 2020, *PASP*, 132, 035001
- Leighly, K. M., Terndrup, D. M., Gallagher, S. C., & Lucy, A. B. 2016, *ApJ*, 829, 4
- Li, Y.-R., Yuan, Y.-F., Wang, J.-M., et al. 2009, *ApJ*, 699, 513
- Li, Y.-R., Wang, J.-M., Ho, L. C., et al. 2016, *ApJ*, 822, 4
- Li, Y.-R., Wang, J.-M., Zhang, Z.-X., et al. 2019, *ApJS*, 241, 33
- Li, Y.-R., Wang, J.-M., Songsheng, Y.-Y. et al. 2022, *ApJ*, arXiv:2201.04470
- Liao, W.-T., Chen, Y.-C., Liu, X. et al. 2021, *MNRAS*, 500, 4025
- Liu, B. F., Meyer, F., Meyer-Hofmeister, E. & Xie, G. Z. 1999, *ApJ*, 527, L17
- Liu, B. F. & Qiao, E. 2022, *iScience*, 25, 103544
- Liu, T., Gezari, S., Ayers, M. et al. 2019, *ApJ*, 884, 36
- Luo, B., Brandt, W. N., Hall, P. B. et al., 2015, *ApJ*, 805, 122
- Mahadevan, R. 1997, *ApJ*, 477, 585
- Manmoto, T. 2000, *ApJ*, 534, 734
- Martin, R. G., Pringle, J. E. & Tout, C. A. 2007, *MNRAS*, 381, 1617
- Mathews, W. G. & Brighenti, F. 2003, *ARA&A*, 41, 191
- Meyer, F. & Meyer-Hofmeister, E. 1994, *A&A*, 228, 175
- Meyer, F. & Meyer-Hofmeister, E. 2002, *A&A*, 392, L5
- Milosavljević, M. & Merritt, D. 2001, *ApJ*, 563, 34
- Montuori, C., Dotti, M., Haardt, F. et al. *MNRAS*, 425, 1633
- Muchotrzeb, B. & Paczyński, B. 1982, *AcA*, 32, 1
- Narayan, R. & Yi, I. 1994, *ApJ*, 428, L13
- Narayan, R. & Yi, I. 1995, *ApJ*, 452, 710
- Ni, Q., Brandt, W. N., Luo, B. et al. 2022, *MNRAS*, 511, 525
- Noble, S. C., Mundim, B. C., Nakano, H., et al. 2012, *ApJ*, 755, 51
- Noble, S. C., Krolik, J. H., Campanelli, M., et al. 2021, *ApJ*, 922, 175
- Nyland, K., Young, L. M., Wrobel, J. M. et al. 2016, *MNRAS*, 458, 2221
- O’Neill, S., Kiehlmann, S., Readhead, A. C. S. et al. 2022, *ApJ*, 926, L35
- Paczyński, B. & Wiita, P. J. 1980, *A&A*, 88, 23

- Paschalidis, V., Bright, J., Ruiz, M. et al. 2021, *ApJ*, 910, L26
- Peters, P. C. 1964, *Phys. Rev.* 136, B1224
- Plotkin R. M., Shemmer, O., Trakhtenbrot, B. et al., 2015, *ApJ*, 805, 123
- Plotkin, R. M., Anderson, S. F., Brandt, W. N., et al. 2010, *ApJ*, 721, 562
- Popović, L. Č., 2012, *New A Rev.*, 56, 74
- Popović, L., Simić, S., Kovacević, A. & Ilić, D. 2021, *MNRAS*, 505, 5192
- Rees, M. J., Begelman, M. C. & Blandford, R. D., 1982, *Nature*, 295, 17
- Runnoe, J. C., Eracleous, M., Pennell, A., et al. 2017, *MNRAS*, 468, 1683
- Sesana, A., Roedig, C., Reynolds, M. T., & Dotti, M. 2012, *MNRAS*, 420, 860
- Shakura, N. I. & Sunyaev, R. 1973, *A&A*, 24, 337
- Shapiro, S. L., Lightman, A. P. & Eardley, D. M. 1976, *ApJ*, 204, 187
- Shen, Y., & Loeb, A. 2010, *ApJ*, 725, 249
- Songsheng, Y.-Y., Wang, J.-M., & Li, Y.-R. 2019, *ApJ*, 883, 184
- Songsheng, Y.-Y., Xiao, M., Wang, J.-M. & Ho, L. C. 2020, *ApJS*, 247, 3
- Stepney, S. & Guibert, P. W. 1983, *MNRAS*, 204, 1269
- Schawinski, K., Koss, M., Berney, S. & Sartori, L. F., 2015, *MNRAS*, 451, 2517
- Valtonen, M. J., Lehto, H. J., Nilsson, K. et al. 2008, *Nature*, 452, 851
- Vaughan, S., Uttley, P., Markowitz, A. G. et al. 2016, *MNRAS*, 461, 3145
- Volonteri, M., Miller, J. M., & Dotti, M. 2009, *ApJ*, 703, L86
- Wang, J.-M., & Li, Y.-R., 2020, *RA&A*, 20, 160
- Wang, J.-M. & Bon, E. 2020, *A&A*, 643, L9
- Wang, J.-M., Songsheng, Y.-Y., Li, Y.-R., Du, P. & Zhang, Z.-X. 2020, *NatAs*, 4, 517
- Wang, J.-M., Songsheng, Y.-Y., Li, Y.-R., & Yu, Z. 2018, *ApJ*, 862, 171
- Wang, J.-M., Watarai, K.-Y. & Mineshige, S. 2004, *ApJ*, 607, L107
- Wang, J.-M. & Zhou, Y.-Y. 1999, *ApJ*, 516, 420
- Wang, J.-M., Szuszkiewicz, E., Lu, F. J. & Zhou, Y.-Y. 1999, *ApJ*, 522, 839
- Welsh, W. F. & Horne, K. 1991, *ApJ*, 379, 586
- Wu, J., Brandt, W. N., Anderson, S. F. et al. 2012, *ApJ*, 747, 10
- Yan, C.-S., Lu, Y., Dai, X., & Yu, Q. 2015, *ApJ*, 809, 117
- Zhang, P., Wang, Z., Gurwell, M. & Wiita, P. J. 2022, *ApJ*, 925, 207
- Zilhaõ, M., Noble, S. C., Campanelli, M., & Zlochower, Y. 2015, *PhRvD*, 91, 024034